Hindawi Publishing Corporation
Mathematical Problems in Engineering
Volume 2012, Article ID 270649, 23 pages
doi:10.1155/2012/270649

Research Article

An Adaptive Variable Structure Control Scheme for Underactuated Mechanical Manipulators

Jung Hua Yang[1] and Kuang Shine Yang[2]

[1] *Department of Vehicle Engineering, National Pingtung University of Science and Technology, Pingtung 91201, Taiwan*
[2] *Department of Mechanical and Electro-Mechanical Engineering, National Sun Yat-sen University, Kaohsiung 80424, Taiwan*

Correspondence should be addressed to Jung Hua Yang, jhyang@mail.npust.edu.tw

Received 10 August 2012; Accepted 20 October 2012

Academic Editor: Zhijian Ji

Mechanical arms have been widely used in the industry for many decades. They have played a dominant role in factory automation. However the control performance, or even system stability, would be deteriorated if some of the actuators fail during the operations. Hence, in this study, an adaptive variable structure scheme is presented to solve this problem. It is shown that, by applying the control mechanism proposed in this paper, the motion of robot systems can maintain asymptotical stability in case of actuators failure. The control algorithms as well as the convergence analysis are theoretically proved based on Lyapunov theory. In addition, to demonstrate the validity of the controller, a number of simulations as well as real-time experiments are also performed for Pendubot robot and Furuta robot systems. The results confirm the applicability of the proposed controller.

1. Introduction

Stabilization and tracking control problems of the nonlinear uncertain underactuated systems are difficult to be dealt with because of their fewer independent control actuators than the degrees of freedom to be controlled. In addition to the lack of enough control inputs for system's degrees of freedom, the dynamics of underactuated mechanical systems is generally characterized by uncertain nonholonomic constraints. And hence, the underactuated system is always a challenging problem in the field of control applications. Robot manipulators have been ubiquitously equipped in many industrial plants for manufacturing automation and most of them were fully actuated. In general, the controller is designed for fully actuated systems based on the properties such as linear controllability, feedback linearizability,

and passivity. However, actuators failure might occur due to infrequent maintenance or limited life cycle, which could cause severe damages to the operators and products. In general, the parts with actuator failures would be unactuated. The underactuated system presents challenging control program since the control design must typically exploit some coupling between the unactuated and the actuated states to achieve the control objective. In this paper, an adaptive variable structure control is presented to obtain globally asymptotical stabilization for a class of underactuated mechanical systems.

Underactuated systems are known as the systems with fewer independent control actuators than the degree of freedom to be controlled. The mathematical representation can be as below:

$$\ddot{q} = f(q, \dot{q}) + b(q)u. \tag{1.1}$$

The system is said to be underactuated if the system satisfies the condition $\operatorname{rank}(b) < \dim(q)$, where q is the state vector of generalized coordinates on the configuration manifold, $\dot{q}$ is the generalized velocity vector, and $b(q)$ is the input state vector.

The underactuated system generally exhibits nonminimum phase [1] and is subject to nonholonomic constraints [2]. In contrast to fully actuated systems controller design, the underactuated system is more difficult with less independent control actuators than the degrees of freedom to be controlled. Tracking control of nonminimum phase systems is a highly sophisticated problem encountered in many practical engineering applications such as rocket control [3], aircraft control [4], flexible link manipulator control [5], and inverted pendulum systems [6]. The nonminimum phase property has long been recognized to be a major obstacle in many control problems. It is well known that unstable zeros cannot be moved with state feedback while the poles can be arbitrarily placed (if completely controllable). For this reason, a growing interest is arising for the design of automatic control systems for the underactuated systems. A lot of literature discussing the control of underactuated systems models has been published in the past years. Wang and other researchers [7, 8] presented a new sliding mode controller for second order underactuated systems. This paper has shown that all sliding surfaces are asymptotically stable. In [9, 10] the authors introduce an IDA-PBC approach to the underactuated mechanical systems. In [11, 12] some nonlinear control schemes, such as feedback linearization, inverse dynamics, and adaptive controller design, have been proposed for the control of underactuated systems. In order to achieve better performance, possibly unknown dynamics must also be considered in control design. In [13], the sliding mode control is proposed to achieve the robustness of many systems such as power systems, electronic motors, and robot manipulators. In [14], the paper provides the state of the art of recent developments in sliding mode control systems with soft computing, examining key technical research issues and future perspectives. In [15], a nonlinear control design is presented, but it requires the solution of a Hamilton-Jacobi type differential equation. It renders the solutions to achieve stability of the system robustly asymptotically stable. The robust backstepping method is utilized to find a stabilizing controller in [16]. The adaptive backstepping controller evolves from [17] with unknown parameters appearing linearly in the state equation, and adaptation mechanism is included to cope with unknown parameters. In [18], the controller is designed for a general class of input-output linearizable systems without zero dynamics, which can be extendable to minimum phase systems. The control scheme uses the backstepping design technique and guarantees semiglobal stability. In paper [19], an adaptive fuzzy output feedback

control approach is proposed for single-input–single-output nonlinear systems without the measurements of the states. It is shown that by applying the proposed adaptive fuzzy control approach, the closed-loop systems are semiglobally uniformly ultimately bounded. In [20], the backstepping technique and adaptive fuzzy backstepping-control approaches for a class of strict-feedback large-scale nonlinear systems with unmodeled dynamics, dynamic disturbances, unknown high-frequency gain signs, and unmeasured states are designed. It has been proved that the proposed adaptive fuzzy control approach can guarantee the uniformly ultimate boundedness of all the signals in the closed-loop system. In [21] a robust adaptive multiestimation-based scheme has been designed for robotic manipulators with force reflection and uncertainties. The closed-loop stability is guaranteed if a minimum residence time, which might be updated online when unknown, between different controller parameterizations is respected. In paper [22], the stable adaptive fuzzy sliding mode controller is developed for nonlinear multivariable systems with unavailable states. It is proved that uniformly asymptotic output feedback stabilization can be achieved. In [23] the authors utilize the coupled sliding mode control concept to achieve the stabilization of inverted pendulum systems. By properly designing the control parameters, the resulting zero dynamics is proved to be semiglobally stable in the presence of bound disturbance.

The paper is organized as follows. In Section 2, an adaptive variable structure control scheme for a class of underactuated mechanical systems is developed. It is verified by computer simulations as well as experiments for the Pendubot system and the Furuta pendulum system, as shown in Sections 3 and 4, respectively. It is observed from both the simulations and the experiments that the effectiveness of the designed controller can be confirmed. Finally, some conclusions are given in Section 5.

2. Adaptive Variable Structure Controller Design

2.1. Problem Formulation

For convenience, the dynamic equations of a general underactuated mechanical manipulator system can be expressed as

$$H(q)\ddot{q} + D(q,\dot{q})\dot{q} + G(q) = u, \tag{2.1}$$

where

$$q = \begin{bmatrix}\theta_1 & \theta_2\end{bmatrix}^T, \qquad u = \begin{bmatrix}\tau \\ 0\end{bmatrix}, \tag{2.2}$$

where q is a vector of n joint displacement, u is the applied torque vector, $H(q) \in R^{n\times n}$ is the effective moment of inertia matrix which is symmetric and positive definite, $\theta_1 \in R^m$ is defined as the actuated joint, $\theta_2 \in R^{n-m}$ denotes the unactuated joint, and m is the number of actuated joint. The centripetal and Coriolis terms collected in the vector $D(q,\dot{q})\dot{q}$ and $G(q)$ represent the gravitational forces.

The dynamic system given in (2.1) exhibits the following properties that are utilized in the subsequent control development and stability analysis.

(P1) The property of $H(q)$ matrices is positive definite and satisfies the following inequalities:

$$Q_1\|\Psi\|^2 \le \xi^T H(q)\xi \le Q_2\|\Psi\|^2, \quad \forall\Psi \in R^n, \tag{2.3}$$

where $Q_1, Q_2 \in R$ are positive constants.

(P2) The property of skew-symmetric matrices satisfies the following relationship:

$$\Psi^T\left(\frac{1}{2}\dot{H}(q) - D(q,\dot{q})\right)\Psi = 0, \quad \forall\Psi \in R^n. \tag{2.4}$$

Equivalently, (2.1) can be rewritten in following partitioned form:

$$\begin{bmatrix} h_{11} & h_{12} \\ h_{21} & h_{22} \end{bmatrix}\begin{bmatrix} \ddot{\theta}_1 \\ \ddot{\theta}_2 \end{bmatrix} + \begin{bmatrix} d_{11} & d_{12} \\ d_{21} & d_{22} \end{bmatrix}\begin{bmatrix} \dot{\theta}_1 \\ \dot{\theta}_2 \end{bmatrix} + \begin{bmatrix} g_1 \\ g_2 \end{bmatrix} = \begin{bmatrix} \tau \\ 0 \end{bmatrix}. \tag{2.5}$$

The control objective in this section is to, for all arbitrary initial conditions, ensure the asymptotical stability of error signal, that is, $\lim_{t\to\infty}\|e\| = 0$. To achieve the tracking control objective, the controller is based on the assumption that $q(t)$, $\dot{q}(t)$ are measurable.

The position tracking error is defined as follows:

$$S = \dot{e} + Ke = \begin{bmatrix} \dot{e}_1 + k_1 e_1 \\ \dot{e}_2 + k_2 e_2 \end{bmatrix} = \begin{bmatrix} s_1 \\ s_2 \end{bmatrix}, \tag{2.6}$$

where $K = \begin{bmatrix} k_1 I_{m\times m} & 0 \\ 0 & k_2 I_{(n-m)\times(n-m)} \end{bmatrix}$ with k_1, k_2 are some designated positive constants. $I_{i\times i}$ is $i \times i$ identity matrix, $e = \begin{bmatrix} e_1 \\ e_2 \end{bmatrix} = \begin{bmatrix} \theta_1 - \theta_1^d \\ \theta_2 - \theta_2^d \end{bmatrix} \in R^n$, and θ_1^d and θ_2^d are the desired trajectories with $\|\theta_1^d\|_\infty \le \varepsilon_1$ and $\|\theta_2^d\|_\infty \le \varepsilon_2$, where $\varepsilon_1, \varepsilon_2$ are some bound positive values and the design of θ_1^d and θ_2^d has to satisfy the zero dynamics $h_{21}\ddot{\theta}_{1d} + h_{22}\ddot{\theta}_{2d} + d_{21}\dot{\theta}_{1d} + d_{22}\dot{\theta}_{2d} + g_2 = 0$. In general, the desired trajectories are often chosen to be constant. Then, in view of (2.5), it is readily obtained that

$$\begin{bmatrix} h_{11} & h_{12} \\ h_{21} & h_{22} \end{bmatrix}\begin{bmatrix} \dot{s}_1 \\ \dot{s}_2 \end{bmatrix} + \begin{bmatrix} d_{11} & d_{12} \\ d_{21} & d_{22} \end{bmatrix}\begin{bmatrix} s_1 \\ s_2 \end{bmatrix} + \begin{bmatrix} k_3 & 0 \\ 0 & k_4 \end{bmatrix}\begin{bmatrix} s_1 \\ s_2 \end{bmatrix} = \begin{bmatrix} W_1\phi_1 + k_3 s_1 + \tau \\ W_2\phi_2 + k_4 s_2 \end{bmatrix} \tag{2.7}$$

or more compactly

$$H(q)\dot{S} + D(q,\dot{q})S + KS = \begin{bmatrix} \mathrm{W}_1\phi_1 + k_3 s_1 + \tau \\ \mathrm{W}_2\phi_2 + k_4 s_2 \end{bmatrix}, \tag{2.8}$$

where

$$W_1\phi_1 = h_{11}\left(-\ddot{\theta}_1^d + x_1\dot{e}_1\right) + h_{12}\left(-\ddot{\theta}_2^d + x_2\dot{e}_2\right) + d_{11}\left(-\dot{\theta}_1^d + x_1e_1\right) + d_{12}\left(-\dot{\theta}_2^d + x_2e_2\right) - g_1,$$
$$W_2\phi_2 = h_{21}\left(-\ddot{\theta}_1^d + x_1\dot{e}_1\right) + h_{22}\left(-\ddot{\theta}_2^d + x_2\dot{e}_2\right) + d_{21}\left(-\dot{\theta}_1^d + x_1e_1\right) + d_{22}\left(-\dot{\theta}_2^d + x_2e_2\right) - g_2, \tag{2.9}$$

$K = \begin{bmatrix} k_3 I_{m\times m} & 0 \\ 0 & k_4 I_{(n-m)\times(n-m)} \end{bmatrix}$ and $k_3 \in R$, $k_4 \in R$ are some positive constants.

2.2. Controller Design

In this subsection, an adaptive variable structure control scheme is presented to account for parameter uncertainty existing in $W_1\phi_1$ and $W_2\phi_2$. From the system dynamics of a robot manipulator with revolute joints, it is well known and can be easily verified that

$$\|W_1\phi_1\| \le \sum_{i=1}^{l} \delta_i Q_i(q,\dot{q}),$$
$$\|W_2\phi_2\| \le \sum_{j=1}^{r} \overline{\sigma}_j \overline{Q}_j(q,\dot{q}), \tag{2.10}$$

where δ_i, $\overline{\sigma}_j$, $i = 1,2,\ldots,l$, $j = 1,2,\ldots,r$ are some unknown positive constants, and $Q_i, \overline{Q}_j$ are known positive functions of q and $\dot{q}$.

Based on the development of the aforementioned error dynamics, the control law is presented as follows:

$$\tau = -k_3 s_1 - \operatorname{sgn}(s_1)\left(\sum_{i=1}^{l} \widehat{\delta}_i Q_i(q,\dot{q})\right) - \operatorname{sgn}(s_1)\|s_2\||\xi| - k_5 \operatorname{sgn}(s_1)\|s_2\|, \tag{2.11}$$

$$\dot{\xi}(t) = \xi^{1/(2n+1)}\left[-k_4\|s_2\|^2 - \|s_2\|\sum_{j=1}^{m} \widehat{\sigma}_j \overline{Q}_j(q,\dot{q})\right], \tag{2.12}$$

where n is some positive integer chosen by designer, k_l, $l = 3,4,5$ are some positive constants, and $\operatorname{sgn}(\cdot)$ is the sign function, which is defined as

$$\operatorname{sgn}(x) = \begin{cases} 1 & x > 0 \\ 0 & x = 0 \\ -1 & x < 0. \end{cases} \tag{2.13}$$

In (2.11) and (2.12) $\widehat{\delta}_i$, $\widehat{\sigma}_j$ denote the parameter estimates, and the estimation errors are defined as follow:

$$\begin{aligned} \widetilde{\delta}_i &= \delta_i - \widehat{\delta}_i, \quad \forall i = 1, \ldots, l, \\ \widetilde{\sigma}_j &= \sigma_j - \widehat{\sigma}_j, \quad \forall j = 1, \ldots, r. \end{aligned} \tag{2.14}$$

Let the parameter estimation laws be designed as

$$\dot{\widehat{\delta}}_i = \Gamma_{ai} \| s_1 \| Q_i(q, \dot{q}), \tag{2.15}$$

$$\dot{\widehat{\sigma}}_j = \Gamma_{bj} \| s_1 \| \overline{Q_j}(q, \dot{q}), \tag{2.16}$$

where $\Gamma_{ai} \in R$, $\Gamma_{bj} \in R$, (for all $i = 1, 2, \ldots, l$, $j = 1, 2, \ldots, r$) are positive definite gain matrices.

Remark 2.1. From the robustness point of view, it would be better if additional feedback term $-k_5 \operatorname{sgn}(s_1)\|s_2\|$ is included in the control law (2.11). With such an inclusion, the stabilization of θ_2 subject to external disturbance can also be maintained as the θ_1 arrived at zero. This can be easily checked from the stability proof given in the theorem.

In the following theorem, it is shown that, by applying the adaptive variable structure controller designed above, the asymptotical stabilization of overall closed-loop system can be achieved.

Theorem 2.2. *Consider the robot system* (2.5) *with imprecise system parameters. By applying the control laws* (2.11)-(2.12) *and estimate laws* (2.15)-(2.16)*, the objective of global asymptotical stabilization can be achieved, that is, all signals inside the close-loop system are bounded and* $e_1, e_2 \to 0$ *asymptotically.*

Proof. To prove the theorem, let the Lyapunov function candidate be defined as

$$V = \frac{1}{2} S^T H S + \frac{1}{2} \sum_{i=1}^{l} \widetilde{\delta}_i^T \Gamma_{ai}^{-1} \widetilde{\delta}_i + \frac{1}{2} \sum_{j=1}^{r} \widetilde{\sigma}_j^T \Gamma_{bj}^{-1} \widetilde{\sigma}_j + \frac{2n+1}{2n} \xi^{2n/(2n+1)} \tag{2.17}$$

and take the time derivative of V to get

$$\begin{aligned} \dot{V} &= S^T H \dot{S} + \frac{1}{2} S^T \dot{H} S + \sum_{i=1}^{l} \widetilde{\delta}_i^T \Gamma_{ai} \dot{\widetilde{\delta}}_i + \sum_{i=1}^{r} \widetilde{\sigma}_j^T \Gamma_{bj} \dot{\widetilde{\sigma}}_i \xi^{-1/(2n+1)} \dot{\xi} \\ &= S^T \left\{ -DS + \begin{bmatrix} \tau + W_1 \phi_1 \\ W_2 \phi_2 \end{bmatrix} \right\} + \frac{1}{2} S^T \dot{H} S + \sum_{i=1}^{l} \widetilde{\delta}_i^T \Gamma_{ai} \dot{\widetilde{\delta}}_i + \sum_{j=1}^{r} \widetilde{\sigma}_j^T \Gamma_{bj} \dot{\widetilde{\sigma}}_i + \xi^{-1/(2n+1)} \dot{\xi} \end{aligned}$$

$$
\begin{aligned}
&= \frac{1}{2}S^T\{\dot{H} - 2D\}S + s_1^T\tau + s_1^T W_1\phi_1 + s_2^T W_2\phi_2 + \sum_{i=1}^{l}\tilde{\delta}_i^T\Gamma_{ai}\dot{\tilde{\delta}}_i + \sum_{j=1}^{r}\tilde{\sigma}_j^T\Gamma_{bj}\dot{\tilde{\sigma}}_i + \xi^{-1/(2n+1)}\dot{\xi} \\
&= s_1^T\tau + s_1^T W_1\phi_1 + s_2^T W_2\phi_2 + \sum_{i=1}^{l}\tilde{\delta}_i^T\Gamma_{ai}\dot{\tilde{\delta}}_i + \sum_{j=1}^{r}\tilde{\sigma}_j^T\Gamma_{bj}\dot{\tilde{\sigma}}_i + \xi^{-1/(2n+1)}\dot{\xi}.
\end{aligned}
\tag{2.18}
$$

In the above derivations, (2.4) has been applied. Then, by using the boundedness of parameter uncertainties (2.10), the time derivative of V can be further expressed as

$$
\begin{aligned}
\dot{V} &\le s_1^T\tau + \|s_1\|\left\|W_1\phi_1\right\| + s_2^T W_2\phi_2 + \sum_{i=1}^{l}\tilde{\delta}_i^T\Gamma_{ai}\dot{\tilde{\delta}}_i + \sum_{j=1}^{r}\tilde{\sigma}_j^T\Gamma_{bj}\dot{\tilde{\sigma}}_i + \xi^{-1/(2n+1)}\dot{\xi} \\
&\le s_1^T\tau + \|s_1\|\sum_{i=1}^{l}\delta_i Q_i(q,\dot{q}) + s_2^T W_2\phi_2 + \sum_{i=1}^{l}\tilde{\delta}_i^T\Gamma_{ai}\dot{\tilde{\delta}}_i + \sum_{j=1}^{r}\tilde{\sigma}_j^T\Gamma_{bj}\dot{\tilde{\sigma}}_i + \xi^{-1/(2n+1)}\dot{\xi}.
\end{aligned}
\tag{2.19}
$$

Thus, by applying the designed controller (2.11)-(2.12) and the adaptive laws (2.15)-(2.16), the following inequality holds:

$$
\begin{aligned}
\dot{V} \le\ & -k_3\|s_1\|^2 + \|s_1\|\|s_2\|\|\xi\| + \|s_2\|\left\|W_2\phi_2\right\| + \sum_{j=1}^{r}\tilde{\sigma}_j^T\Gamma_{bj}\dot{\tilde{\sigma}}_i + \xi^{-1/(2n+1)}\dot{\xi} - k_5|s_1|\|s_2\| \\
\le\ & -k_3\|s_1\|^2 - \|s_1\|\|s_2\|\|\xi\| + \|s_2\|\sum_{j=1}^{m}\delta_j\overline{Q}_j(q,\dot{q}) + \sum_{j=1}^{r}\tilde{\sigma}_j^T\Gamma_{bj}\left(-\Gamma_{bj}\|s_2\|\overline{Q}_j(q,\dot{q})\right) \\
& + \xi^{-1/(2n+1)}\dot{\xi} - k_5|s_1|\|s_2\| \\
\le\ & -k_3\|S_1\|^2 - \|S_1\|\|S_2\|\|\xi\| + \|S_2\|\sum_{j=1}^{m}\delta_j\overline{Q}_j(q,\dot{q}) + \sum_{j=1}^{r}\tilde{\sigma}_j^T\Gamma_{bj}\left(-\Gamma_{bj}\|S_2\|\overline{Q}_j(q,\dot{q})\right) \\
& + \left[-k_4\|S_2\|^2 - \|S_2\|\sum_{j=1}^{m}\hat{\sigma}\overline{Q}_j(q,\dot{q})\right] - k_5|s_1|\|s_2\| \\
\le\ & -k_3\|S_1\|^2 - k_4\|S_2\|^2 - \|S_1\|\|S_2\|\|\xi\| - k_5|s_1|\|s_2\| \\
\le\ & -\|S\|^T K\|S\|,
\end{aligned}
\tag{2.20}
$$

where $K = \begin{bmatrix} k_3 & 0 \\ 0 & k_4 \end{bmatrix}$. Thus, it is clear that $\dot{V}(t) \le 0$ if $k_3, k_4, k_5 > 0$. Then, according to Barbalat's lemma [22], it is readily obtained that $S \to 0$ as $t \to \infty$ asymptotically and, hence, $e, \dot{e} \to 0$ as $t \to \infty$. □

In the next section, the Pendubot system and the Furuta pendulum system are studied to verify the above theoretical results.

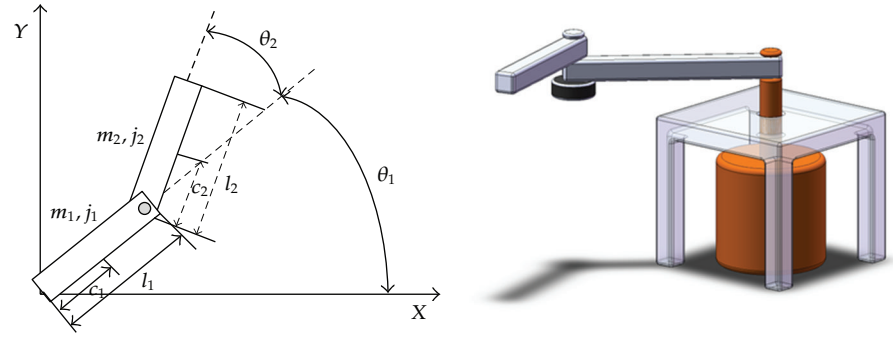

(a) (b)

Figure 1: The Pendubot system.

3. Applications to the Pendubot System

In this section, the adaptive sliding mode control scheme developed previously is applied to the Pendubot system. The Pendubot system is a two link planner manipulator in which the first link is driven by an actuator but the second link is unactuated, as shown in Figure 1. Link 1 and link 2 are connected by revolute joint, and link 1 can freely rotate about 360 degrees in the horizontal plane. In this section, the kinematic and dynamic models of a Pendubot system are presented.

The equation of motion is derived using Lagrange's equation [24] as

$$\frac{d}{dt}\left(\frac{\partial L}{\partial \dot{q}}(q,\dot{q})\right) - \frac{\partial L}{\partial \dot{q}}(q,\dot{q}) = \tau. \tag{3.1}$$

The Lagrange's function is given by

$$L = K - P, \tag{3.2}$$

where K is the kinetic energy of the system and P is The potential energy of the system.

From the Lagrange's equation, it is shown that the equation of motion for this system can be represented in the following form:

$$M(q)\ddot{q} + C(q,\dot{q})\dot{q} = \tau, \tag{3.3}$$

$M(q) \in R^{n\times n}$ is the inertia matrix, $C(q,\dot{q}) \in R^{n\times n}$ is the centripetal-Coriolis matrix.

Where $q(t) \in R^2$ is the joint position defined as follows:

$$q = \begin{bmatrix}\theta_1 & \theta_2\end{bmatrix}, \tag{3.4}$$

where $\theta_1 \in R^1$ and $\theta_2 \in R^1$ denote the angles of link 1 and link 2, respectively. $M(q) \in R^{2\times 2}$, $C(q,\dot{q}) \in R^{2\times 2}$, and control input vector τ are defined as follows:

$$q = \begin{bmatrix}\theta_1\\ \theta_2\end{bmatrix}, \qquad M(q) = \begin{bmatrix}m_{11} & m_{12}\\ m_{21} & m_{22}\end{bmatrix}, \qquad C(q,\dot{q}) = \begin{bmatrix}c_{11} & c_{12}\\ c_{21} & c_{22}\end{bmatrix}, \qquad \tau = \begin{bmatrix}u\\ 0\end{bmatrix}, \tag{3.5}$$

where

$$\begin{aligned}
m_{11} &= m_1 {c_1}^2 + m_2 {l_1}^2 + m_2 {c_2}^2 + 2m_2 l_1 c_2 \cos\theta_2 + J_1 + J_2,\\
m_{12} &= m_2 {c_2}^2 + m_2 l_1 c_2 \cos\theta_2 + J_2,\\
m_{21} &= m_2 {c_2}^2 + m_2 l_1 c_2 \cos\theta_2 + J_2,\\
m_{22} &= m_2 {c_2}^2 + J_2,\\
c_{11} &= -m_2 l_1 c_2 \dot{\theta}_2 \sin\theta_2,\\
c_{12} &= -m_2 l_1 c_2 \dot{\theta}_1 \sin\theta_2 - m_2 l_1 c_2 \dot{\theta}_2 \sin\theta_2,\\
c_{21} &= m_2 l_1 c_2 \dot{\theta}_1 \sin\theta_2,\\
c_{22} &= 0.
\end{aligned} \tag{3.6}$$

From (3.1), as mentioned above, the inertia and centripetal-Coriolis matrices satisfy the following condition:

$$\Psi^T \left(\frac{1}{2}\dot{M}(q) - D(q,\dot{q})\right)\Psi = 0, \tag{3.7}$$

where

$$\dot{M}(q) - 2D(q,\dot{q}) = \begin{bmatrix} 0 & m_2 l_1 c_2 \sin q_2 \left(2\dot{q}_1 + \dot{q}_2\right)\\ -m_2 l_1 c_2 \sin q_2 \left(2\dot{q}_1 + q_2\right) & 0\end{bmatrix} \tag{3.8}$$

which is a skew-symmetric matrix. The system variables and parameters are defined in Table 1.

As described in the preceding section, the adaptive variable structure controller will be adopted to drive the first link to the desired position, and keep the second link to settle down at the original angle. From the dynamic equation shown above, the following bounding assumption can be made for $W_1\phi_1$ and $W_2\phi_2$:

$$\begin{aligned}
\left\|W_1\phi_1\right\| &\le \delta_1\left(\dot{\theta}_1^2 + \dot{\theta}_2^2\right) + \delta_2\left({e_1}^2 + {e_2}^2\right) + \delta_3,\\
\left\|W_2\phi_2\right\| &\le \sigma_1\left(\dot{\theta}_1^2 + \dot{\theta}_2^2\right) + \sigma_2 {e_1}^2 + \sigma_3,
\end{aligned} \tag{3.9}$$

Table 1: Definitions of system variables and parameters.

m_1: mass of link 1 (0.056 kg)
m_2: mass of link 2 (0.022 kg)
l_1: length of link 1 (0.16 m)
l_2: length of link 2 (0.16 m)
c_1: distance to link 1 center of mass (0.08 m)
c_2: distance to link 2 center of mass (0.08 m)
J_1: inertia of link 1 (0.001569 kg·m^2)
J_2: inertia of link 2 (0.001785 kg·m^2)
θ_1: displacement of link 1
$\dot{\theta}_1$: angular velocity of link 1
θ_2: displacement of link 2
$\dot{\theta}_2$: angular velocity of link 2
τ_l: applied torque

where δ_i, $i = 1,2,3$ and σ_j, $j = 1,2,3$ are unknown positive bounded constants. Before proceeding with the adaptive sliding mode control design, let the parameter estimation errors be defined as

$$\begin{aligned} \widetilde{\delta}_i &= \delta_i - \widehat{\delta}_i, \quad i = 1,2,3, \\ \widetilde{\sigma}_j &= \sigma_j - \widehat{\sigma}_j, \quad j = 1,2,3. \end{aligned} \tag{3.10}$$

From the error dynamics (2.7), the adaptive controllers can be designed as

$$\begin{aligned} u &= -k_3 s_1 - \operatorname{sgn}(s_1)\left(\widehat{\delta}_1\left(\dot{\theta}_1^2 + \dot{\theta}_2^2\right) + \widehat{\delta}_2\left(e_1^2 + e_2^2\right) + \widehat{\delta}_3\right) - \operatorname{sgn}(s_1)|s_2||\xi| - k_5 \operatorname{sgn}(s_1)\|s_2\|, \\ \dot{\xi}(t) &= \xi^{1/(2n+1)}\left[-k_4 s_2^2 - |s_2|\left(\widehat{\sigma}_1\left(\dot{\theta}_1^2 + \dot{\theta}_2^2\right) + \widehat{\sigma}_2 e_1^2 + \widehat{\sigma}_3\right)\right], \end{aligned} \tag{3.11}$$

with the adaptive laws

$$\dot{\widehat{\delta}}_1 = \Gamma_{11}|s_1|\left(\dot{\theta}_1^2 + \dot{\theta}_2^2\right), \tag{3.12}$$

$$\dot{\widehat{\delta}}_2 = \Gamma_{12}|s_1|\left(e_1^2 + e_2^2\right), \tag{3.13}$$

$$\dot{\widehat{\delta}}_3 = \Gamma_{13}|s_1|, \tag{3.14}$$

$$\dot{\widehat{\sigma}}_1 = \Gamma_{21}|s_2|\left(\dot{\theta}_1^2 + \dot{\theta}_2^2\right), \tag{3.15}$$

$$\dot{\widehat{\sigma}}_2 = \Gamma_{22}|s_2|e_1^2, \tag{3.16}$$

$$\dot{\widehat{\sigma}}_3 = \Gamma_{23}|s_2|, \tag{3.17}$$

where Γ_{ij}, $i = 1,2$, $j = 1,2,3$ are positive constants.

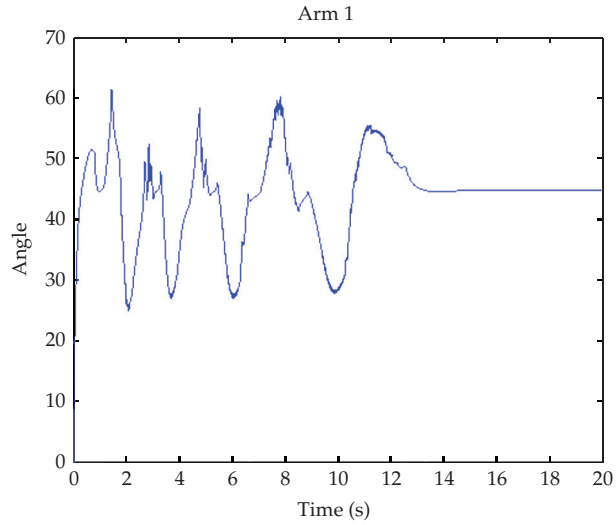

Figure 2: Link 1 angular displacement with adaptive algorithm.

3.1. Simulation Results

A number of simulations are performed for the adaptive sliding mode schemes proposed in this section. In this simulation, the initial positions of link 1 and link 2 are identically 0°. The desired final position for link 1 is $\theta_1^d = 45°$ and for link 2 is $\theta_2^d = 0°$, respectively.

The simulation results are shown in Figures 2–6. Figures 2 and 3 show the link 1 output angle and link 2 output angle responses, respectively. It is seen that link 1 and link 2 can converge to the target in 16 seconds. Figure 4 shows the convergence of the adaptive laws, while Figure 5 shows the control adaptation gain parameters $\xi(t)$. Finally, the control input is shown in Figures 6 and 12. The control gains used in the simulation are chosen to be $k_1 = 0.3$, $k_2 = 20$, $k_3 = 1.3$, and $k_4 = 70$, and the adaptive gains are chosen as $\Gamma_{11} = 0.1$, $\Gamma_{12} = 1$, $\Gamma_{13} = 0.01$, $\Gamma_{21} = 1$, $\Gamma_{22} = 1$, and $\Gamma_{23} = 1$.

3.2. Experimental Results

To validate the practical application of the proposed algorithm experiments on the underactuated mechanical system apparatus is also conducted, as shown in Figure 7. In the mechanical system the actuator is dc motor mounted on the arm (link 1) and coupled to links through the power MOSFET chopper amplifier. A 500 pulse/rev shaft encoder is used to sense the arm (link 1) position and pendulum position or link 2 position. A 12 bit A/D converter provides the required signal. The microcomputer used is a INTEL-P4-based system with 3 GHz clock.

To demonstrate the effectiveness of our proposed controller, a comparison with the results in [23] is made. The controller gains are chosen to be $k = 10$, $c_x = 1$, and $c_\theta = 2$ and the results are depicted in Figures 8 and 9. In the experiment, the desired final position for link 1 is $\theta_1^d = 45°$, and for link 2 is $\theta_2^d = 0°$. From Figure 10 it is seen that link 1 could converge to 23 degrees at nearly 5 seconds but link 2 couldn't keep at 0 degree as indicated in Figure 11. From the experimental results, it is clearly observed that even though the exact

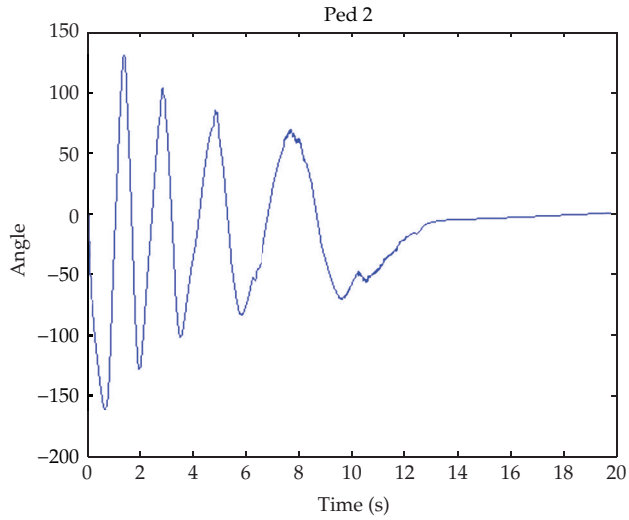

Figure 3: Link 2 angular displacement with adaptive algorithm.

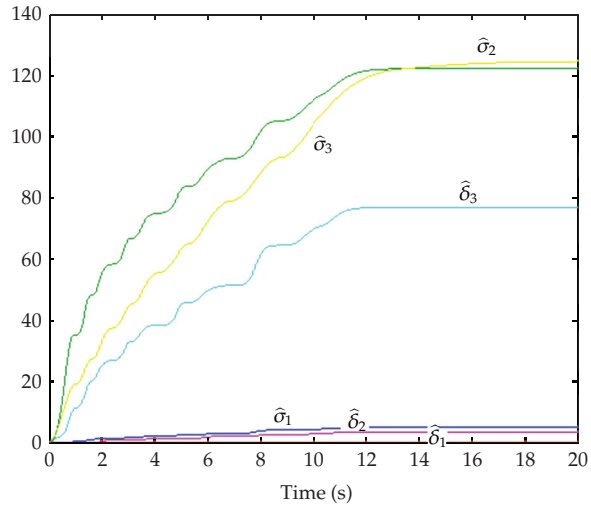

Figure 4: Adaptive control gains estimates for the controller.

dynamics of the nonlinear model is available but with the system parameter unknown, the control precision is still a problem needed to be solved.

For the experiment by using the controller proposed in this paper, the same conditions as above are set, $\theta_1^d = 45°$ for link 1 and $\theta_2^d = 0$ for link 2. For the controller proposed in this paper, the following controlled gains are chosen for experiments: $k_1 = 10$, $k_2 = 4$, $k_3 = 1$, and $k_4 = 1$, and the adaptive gains are set to be $\Gamma_{11} = \Gamma_{12} = \Gamma_{13} = \Gamma_{21} = \Gamma_{22} = \Gamma_{23} = 0.1$. Figures 10 and 11 depict the position response of link 1 and link 2, and from the figures it is observed that link 1 converges to the target nearly in 2 seconds, while the convergence of link 2 is completed in 6 seconds. The control input is described in Figure 14. It is seen that the adaptive controller can provide stable and better performance over a wide range of parameter variations in comparison with the conventional sliding mode controller.

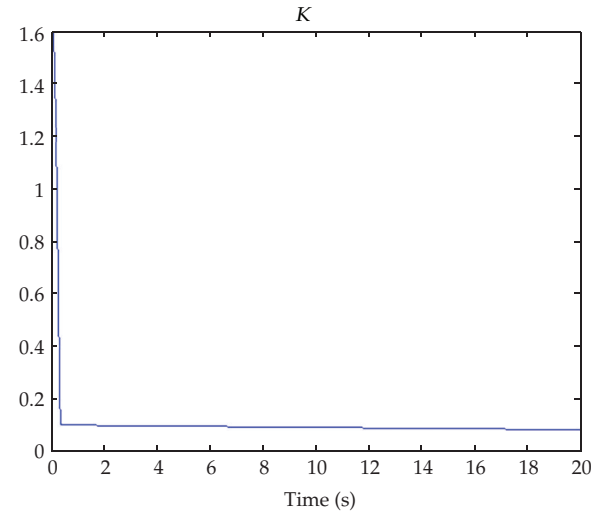

Figure 5: The control gain $\xi(t)$ estimate for the adaptive controller.

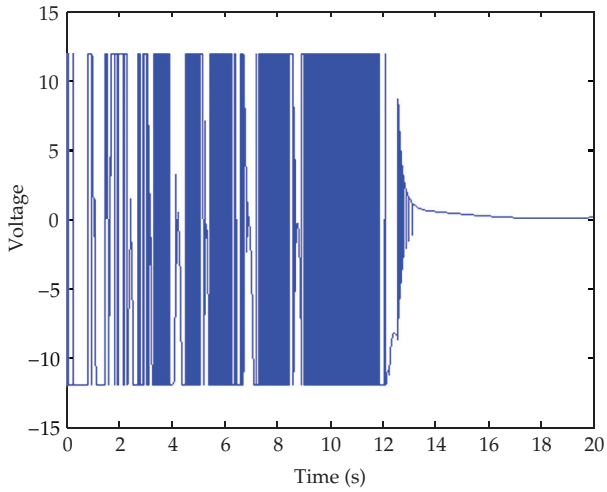

Figure 6: Control input voltage for the adaptive controller.

4. Applications to the Furuta Pendulum System

In this section, the Furuta pendulum system [1] is considered for demonstration. Figure 13 illustrates the mechanical system.

The equation of motion can be written in the following general form:

$$M(q)\ddot{q} + D(q,\dot{q})\dot{q} + G(q) = \begin{bmatrix} \tau_l \\ 0 \end{bmatrix}, \tag{4.1}$$

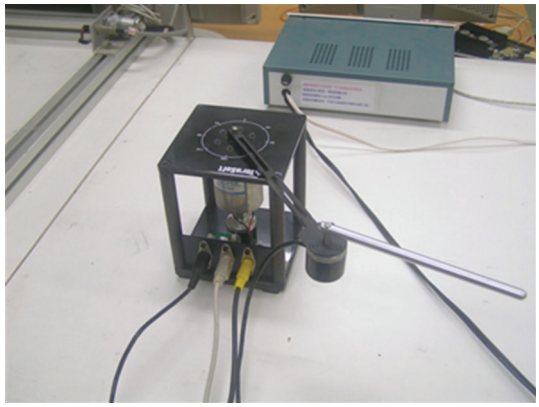

Figure 7: Experimental setup for Pendubot system.

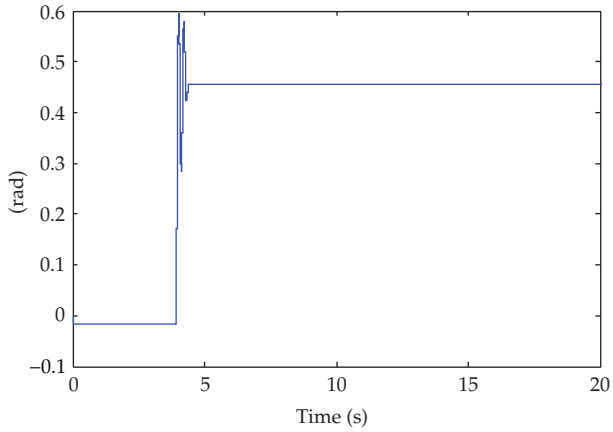

Figure 8: Link 1 angular displacement (compared sliding mode controller).

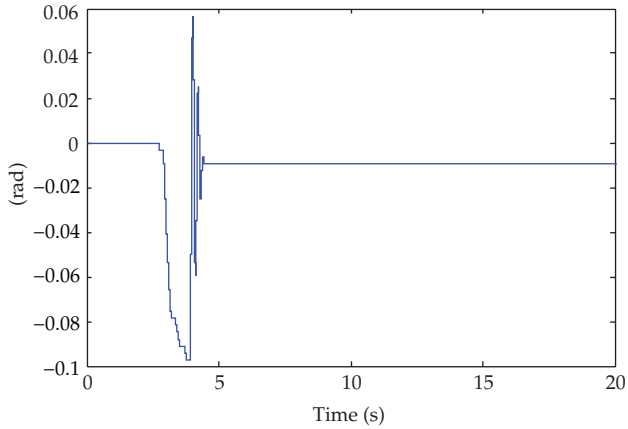

Figure 9: Link 2 angular displacement (compared sliding mode controller).

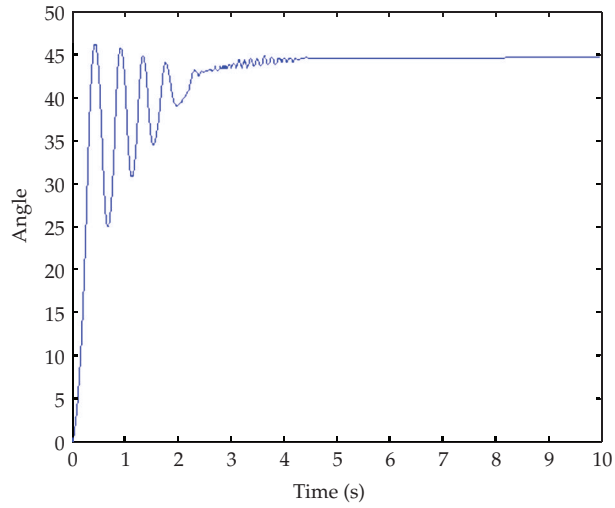

Figure 10: Link 1 angular displacement with adaptive algorithm.

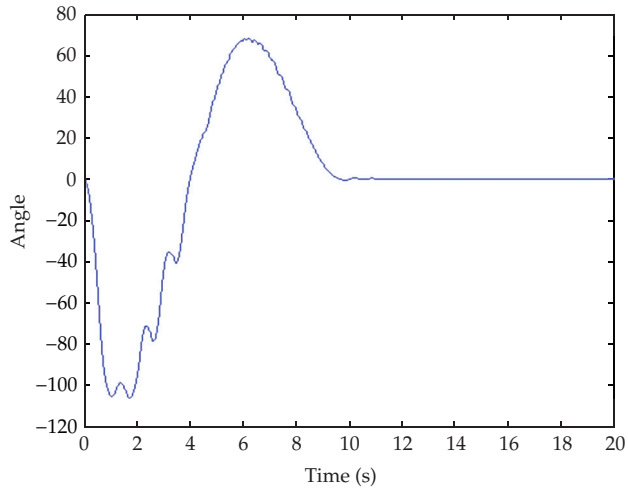

Figure 11: Link 2 angular displacement with adaptive algorithm.

where

$$M(q) = \begin{bmatrix} I_0 + m_1\left(L_0^2 + l_1^2 \sin^2\theta_2\right) & m_1 L_0 l_1 \cos\theta_2 \\ m_1 l_1 L_0 \cos\theta_2 & J_1 + m_1 l_1^2 \end{bmatrix},$$

$$D(q,\dot{q}) = \begin{bmatrix} \frac{1}{2} m_2 l_1^2 \dot{\theta}_2 \sin(2\theta_2) & -m_1 l_1 L_0 \dot{\theta}_2 \sin\theta_2 + \frac{1}{2} m_1 l_1^2 \dot{\theta}_1 \sin(2\theta_2) \\ -\frac{1}{2} m_1 l_1^2 \dot{\theta}_1 \sin(2\theta_2) & 0 \end{bmatrix}, \tag{4.2}$$

$$G(q) = \begin{bmatrix} 0 \\ -m_1 l_1 g \sin\theta_2 \end{bmatrix}.$$

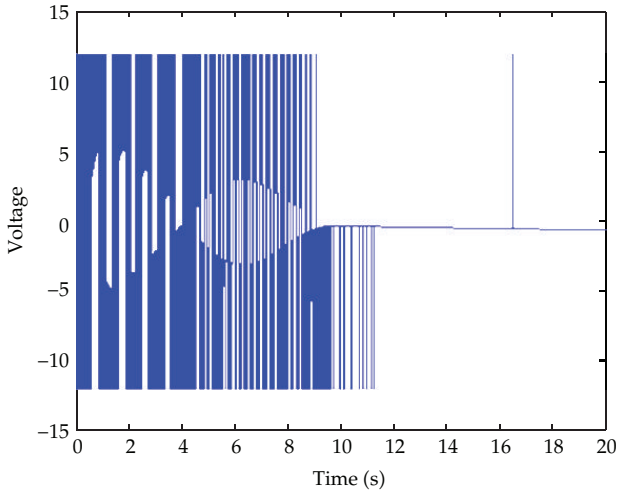

Figure 12: Control input voltage for the adaptive controller.

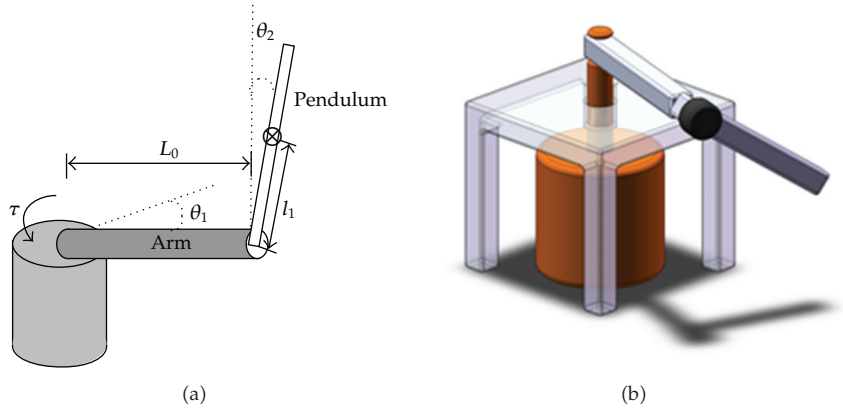

Figure 13: The Furuta pendulum system.

Form (3.14)-(3.15), it is straightforward to show that the following relationship is satisfied:

$$\Psi^T \left(\frac{1}{2} \dot{M}(q) - D(q, \dot{q}) \right) \Psi = 0. \tag{4.3}$$

Clearly, $\dot{M}(q) - 2D(q, \dot{q}) = \begin{bmatrix} 0 & -m_1 l_1 (l_1 \sin(2\theta_2)\dot{\theta}_1) - L_0 \sin\theta_2 \dot{\theta}_2 \\ m_1 l_1 (l_1 \sin(2\theta_2)\dot{\theta}_1) - L_0 \sin\theta_2 \dot{\theta}_2 & 0 \end{bmatrix}$ is a skew-symmetric matrix. The system variables and parameters are defined in Table 2.

Table 2: Definitions of system variables and parameters for Furuta pendulum system.

I_0: inertia of the arm ($I_0 = 0.001569\,\text{kg}\cdot\text{m}^2$)
L_0: total length of the arm ($L_0 = 0.16\,\text{m}$)
m_1: mass of the arm ($m_1 = 0.056\,\text{kg}$)
m_2: mass of the pendulum ($m_1 = 0.022\,\text{kg}$)
l_1: distance to the center of gravity of the pendulum ($l_1 = 0.08\,\text{m}$)
J_1: inertia of the pendulum around its center of gravity ($J_1 = 0.0001785\,\text{kg}\cdot\text{m}^2$)

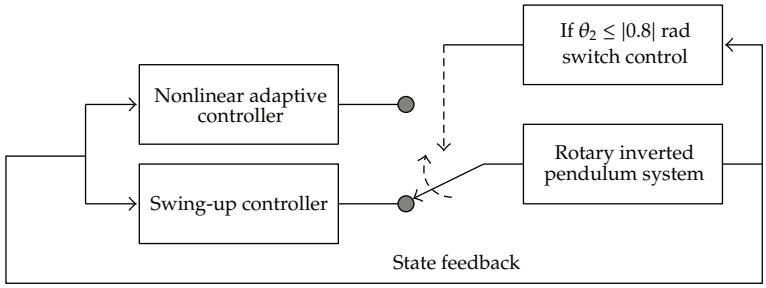

Figure 14: Control Structure.

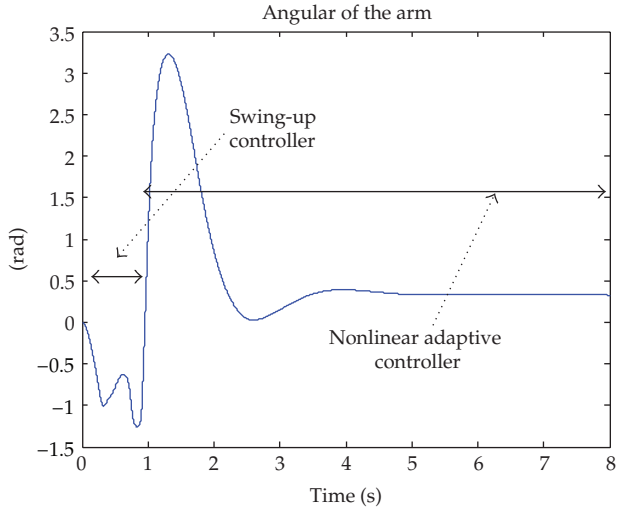

Figure 15: Link 1 angular displacement with adaptive algorithm.

Stage 1 (Swing up the Pendulum). The control objective here is to move the pendulum from the stable equilibrium position to the unstable equilibrium position. In order to balance the pendulum to the unstable equilibrium point, a swing-up controller should be first applied to make the pendulum inside some acceptable region around the vertical line. Then, the adaptive controller will be activated to keep the pendulum upright at the unstable equilibrium point.

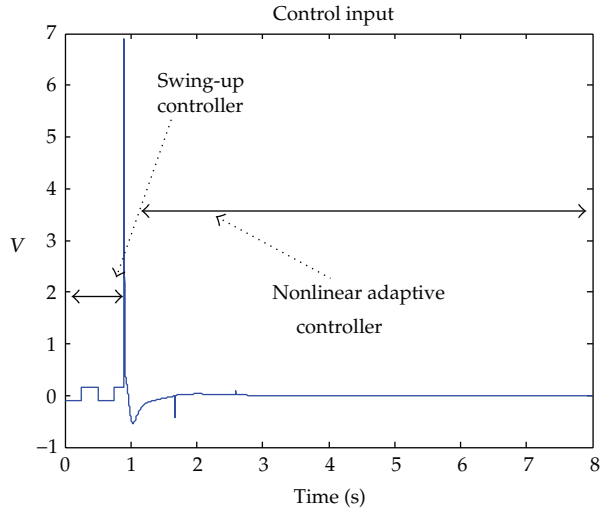

Figure 16: Control input voltage for the adaptive controller.

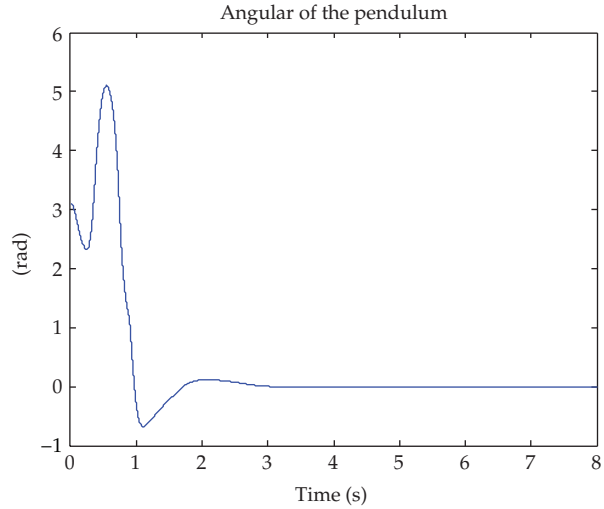

Figure 17: Link 2 angular displacement with adaptive algorithm.

The swing-up control law can be written as

$$u_s(t) = \begin{cases} 0, & t = 0, \\ c_1, & t_{i+1} > t_i > 0, \\ -c_2, & t_{i+2} > t_{i+1}, \end{cases} \tag{4.4}$$

where c_1, c_2 are positive constants.

As shown in Figure 14, when the pendulum is within ±0.8 rad of the vertical position, the balancing controller is activated. Otherwise, the system operates under swing-up control.

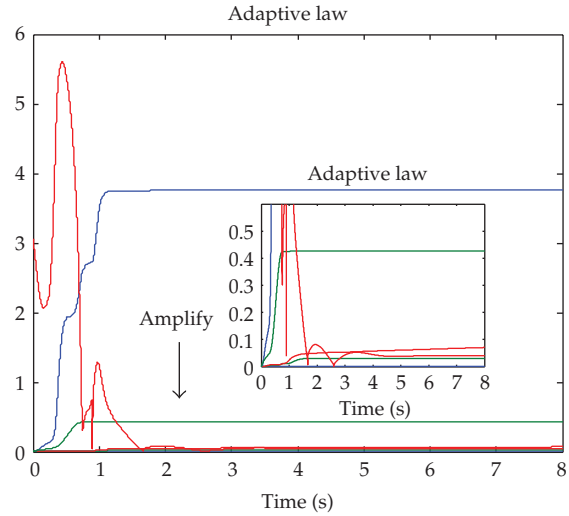

Figure 18: Adaptive control gains estimates for the controller.

Stage 2 (Balance the Pendulum). Form the dynamic equation shown above, it is found that bounds of $W_1\phi_1$ and $W_2\phi_2$ can be written as

$$\begin{aligned} \|W_1\phi_1\| &\le \delta_1\left(\dot{\theta}_1^2+\dot{\theta}_2^2\right)+\delta_2\left(e_1^2+e_2^2\right)+\delta_3, \\ \|W_2\phi_2\| &\le \sigma_1\left(\dot{\theta}_1^2+\dot{\theta}_2^2\right)+\sigma_2 {e_1}^2+\sigma_3. \end{aligned} \tag{4.5}$$

The controller and adaptive gain are designed as follows:

$$\begin{aligned} u &= -k_3 s_1-\operatorname{sgn}(s_1)\left(\widehat{\delta}_1\left(\dot{\theta}_1^2+\dot{\theta}_2^2\right)+\widehat{\delta}_2\left(e_1^2+e_2^2\right)+\widehat{\delta}_3\right)-\operatorname{sgn}(s_1)|s_2||\xi|-k_5 s_2, \\ \dot{\xi}(t) &= \xi^{1/(2n+1)}\left[-k_4 s_2^2-|s_2|\left(\widehat{\sigma}_1\left(\dot{\theta}_1^2+\dot{\theta}_2^2\right)+\widehat{\sigma}_2 e_1^2+\widehat{\sigma}_3\right)\right]. \end{aligned} \tag{4.6}$$

The adaptive laws is as follows:

$$\begin{aligned} \dot{\widehat{\delta}}_1 &= \Gamma_{11}|s_1|\left(\dot{\theta}_1^2+\dot{\theta}_2^2\right), \\ \dot{\widehat{\delta}}_2 &= \Gamma_{12}|s_1|\left(e_1^2+e_2^2\right), \\ \dot{\widehat{\delta}}_3 &= \Gamma_{13}|s_1|, \\ \dot{\widehat{\sigma}}_1 &= \Gamma_{21}|s_2|\left(\dot{\theta}_1^2+\dot{\theta}_2^2\right), \\ \dot{\widehat{\sigma}}_2 &= \Gamma_{22}|s_2|e_1^{2,} \\ \dot{\widehat{\sigma}}_3 &= \Gamma_{23}|s_2|, \end{aligned} \tag{4.7}$$

where Γ_{ij}, $i=1,2$, $j=1,2,3$ are positive constants.

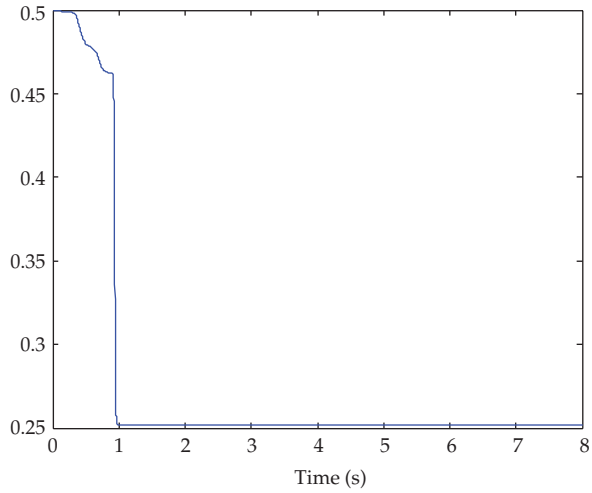

Figure 19: The control gain $\xi(t)$ estimate for the adaptive controller.

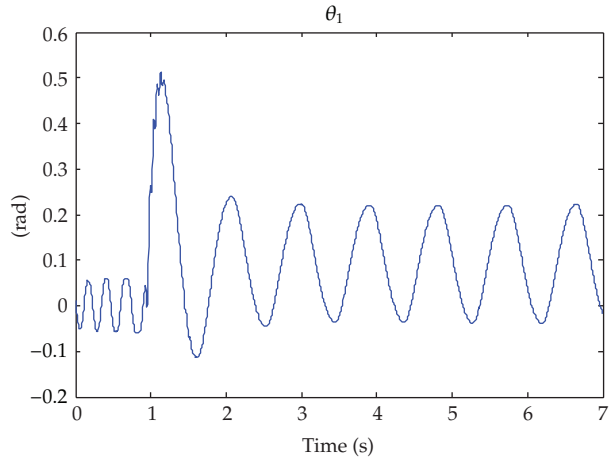

Figure 20: Link 1 angular displacement (sliding mode controller).

4.1. Simulation Results

The simulations are performed using MATLAB and SIMULINK to show the validity of the controller. The results are indicated in Figures 15–4.

In the simulations, the initial positions of θ_1 and θ_2 are chosen identically as 0°. The desired arm position and pendulum position are chosen as $\theta_1^d = 0.4\,\text{rad}$, as $\theta_2^d = 0\,\text{rad}$, respectively. As illustrated in Figure 15 the steady state position tracking error can approach to zero in 6 seconds. As the results in Figure 4 show, the tracking error of unactuated link can converge stably in a fast manner, and it is observed that all the parameter estimates trajectories are convergent, as shown in Figure 18. The control input is shown in Figure 16. Figure 4 plots the trajectory of $\xi(t)$.

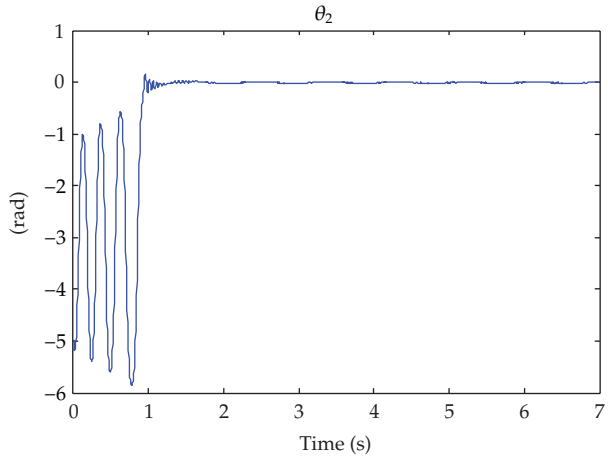

Figure 21: Link 2 angular displacement (sliding mode controller).

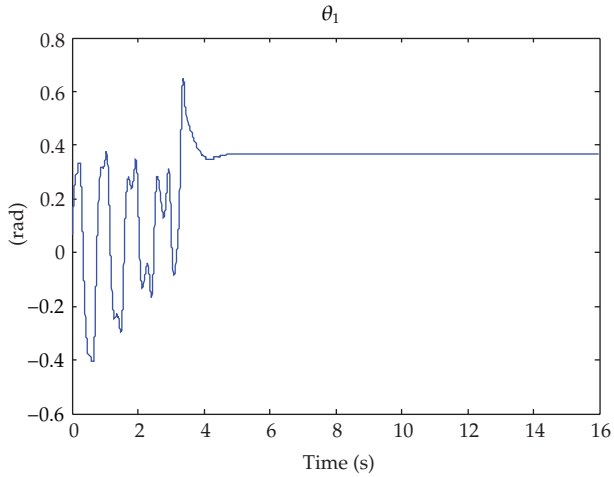

Figure 22: Link 1 angular displacement with adaptive algorithm.

4.2. *Experimental Results*

Similarly, the results obtained from the sliding mode controller [23] and the adaptive controller proposed in this paper are also performed and compared in Figures 22–24. From Figures 20 and 4.1 it is seen that, although the pendulum converge to target, the arm could not precisely settle down to its desired position but oscillates within some bounded region by using the sliding mode controller. It means that the poor closed-loop system response might arise due to system parameters.

As for the experiment of adaptive controller, the controlled gains are chosen as $k_1 = 1$, $k_2 = 0.5$, $k_3 = 10$, and $k_4 = 1$. The corresponding adaptive gains are set to be $\Gamma_{11} = \Gamma_{12} = \Gamma_{13} = \Gamma_{21} = \Gamma_{22} = \Gamma_{23} = 0.01$. In this experiment, the control gains are difficult to determine due to the unknown uncertainties in practical applications and are generally chosen as a compromise between the stability and the control performance. Figures 22 and 23 depict the position response of arm and pendulum. It is observed from the figures that the arm could

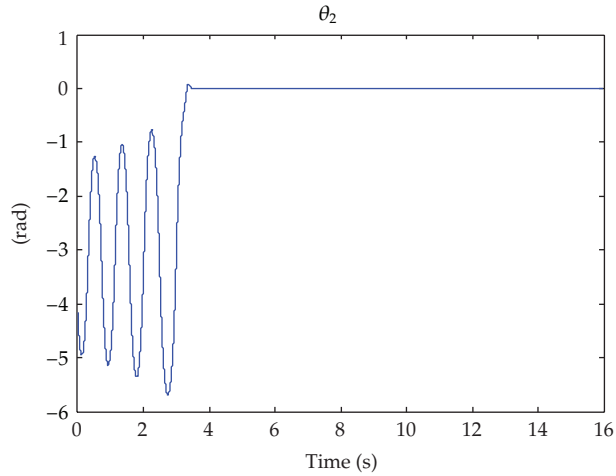

Figure 23: Link 2 angular displacement with adaptive algorithm.

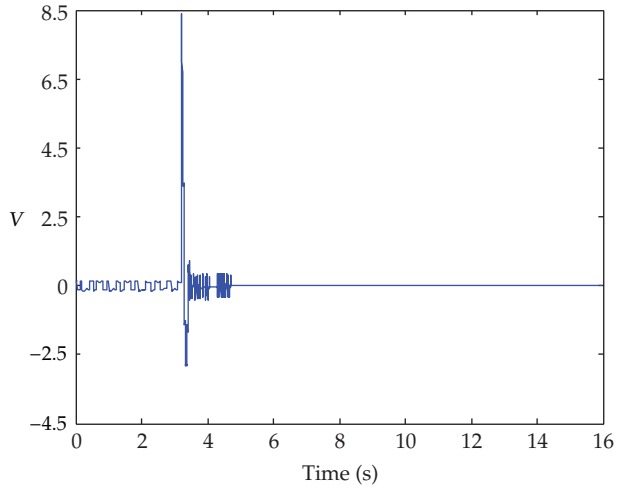

Figure 24: Control input voltage for the adaptive controller.

converge to the desired position at 6 sec with the pendulum swinging up to top position in 5 seconds. Finally the control input is described in the Figure 24.

5. Conclusion

In this paper, the adaptive control for underactuated mechanical systems with parameter uncertainty is discussed. By utilizing Lyapunov-based stability analysis asymptotical stabilization of such systems can be guaranteed. The control schemes are also implemented in the Pendubot system and Furuta pendulum system to verify the performance of the proposed adaptive sliding controller. It is shown that the tracking error can be made asymptotically stable undergoing such controller design.

References

[1] I. Fantoni and R. Lozano, *Non-Linear Control for Underactuated Mechanical Systems*, Springer, 2002.

[2] A. M. Bloch, *Nonholonomic mechanics and control*, vol. 24 of *Interdisciplinary Applied Mathematics*, Springer, New York, NY, USA, 2003.

[3] J. Hu and C. Huang, "Simulation on multiple impulse correction control system of rockets," in *Proceedings of the IEEE International Conference on Mechatronics and Automation (ICMA '07)*, pp. 1518–1522, August 2007.

[4] Y. J. Huang, T. C. Kuo, and H. K. Way, "Robust vertical takeoff and landing aircraft control via integral sliding mode," *IEE Proceedings*, vol. 150, no. 4, pp. 383–388, 2003.

[5] F. M. C. Ching and D. Wang, "Exact solution and infinite-dimensional stability analysis of a single flexible link in collision," *IEEE Transactions on Robotics and Automation*, vol. 19, no. 6, pp. 1015–1020, 2003.

[6] S. Awtar, N. King, T. Allen et al., "Inverted pendulum systems: rotary and arm-driven—a mechatronic system design case study," *Mechatronics*, vol. 12, no. 2, pp. 357–370, 2002.

[7] W. Wang, J. Yi, D. Zhao, and D. Liu, "Design of a stable sliding-mode controller for a class of second-order underactuated systems," *IEE Proceedings*, vol. 151, no. 6, pp. 683–690, 2004.

[8] Y. Hao, J. Yi, D. Zhao, and W. Wang, "Proposal of incremental sliding mode control," in *Proceedings of the 1st International Conference on Innovative Computing, Information and Control (ICICIC '06)*, pp. 340–343, September 2006.

[9] J. Acosta, R. Ortega, A. Astolfi, and A. D. Mahindrakar, "Interconnection and damping assignment passivity-based control of mechanical systems with underactuation degree one," *IEEE Transactions on Automatic Control*, vol. 50, no. 12, pp. 1936–1955, 2005.

[10] R. Ortega, M. W. Spong, F. Gómez-Estern, and G. Blankenstein, "Stabilization of a class of underactuated mechanical systems via interconnection and damping assignment," *IEEE Transactions on Automatic Control*, vol. 47, no. 8, pp. 1218–1233, 2002.

[11] J. Hauser, S. Sastry, and P. Kokotović, "Nonlinear control via approximate input-output linearization: the ball and beam example," *IEEE Transactions on Automatic Control*, vol. 37, no. 3, pp. 392–398, 1992.

[12] K. S. Narendra and A. M. Annaswamy, *Stable Adaptive Systems*, Prentice Hall, 1989.

[13] V. I. Utkin, *Sliding Modes in Control and Optimization*, Communications and Control Engineering Series, Springer, Berlin, Germnay, 1992.

[14] X. Yu and O. Kaynak, "Sliding-mode control with soft computing: a survey," *IEEE Transactions on Industrial Electronics*, vol. 56, no. 9, pp. 3275–3285, 2009.

[15] A. van der Schaft, *L_2 Gain and Passivity Techniques in Nonlinear Control*, Springer, 1996.

[16] R. Sepulchre, M. Jankovic, and P. Kokotovic, *Constructructive Nonlinear Control*, Springer, 1997.

[17] M. Krstic, I. Kanellakopoulos, and P. Kokotovic, *Nonlinear and Adaptive Control Design*, John Wiley & Sons, 1995.

[18] Y. Zhang and P. Y. Peng, "Stable neural controller design for unknown nonlinear systems using backstepping," in *Proceedings of the American Control Conference*, pp. 1067–1071, June 1999.

[19] S. C. Tong, X. L. He, and H. G. Zhang, "A combined backstepping and small-gain approach to robust adaptive fuzzy output feedback control," *IEEE Transactions on Fuzzy Systems*, vol. 17, no. 5, pp. 1059–1069, 2009.

[20] S. Tong, C. Liu, and Y. Li, "Fuzzy-adaptive decentralized output-feedback control for large-scale nonlinear systems with dynamical uncertainties," *IEEE Transactions on Fuzzy Systems*, vol. 18, no. 5, pp. 845–861, 2010.

[21] A. Ibeas and M. de la Sen, "Robustly stable adaptive control of a tandem of master-slave robotic manipulators with force reflection by using a multiestimation scheme," *IEEE Transactions on Systems, Man, and Cybernetics, Part B*, vol. 36, no. 5, pp. 1162–1179, 2006.

[22] S. Tong and H. X. Li, "Fuzzy adaptive sliding-mode control for MIMO nonlinear systems," *IEEE Transactions on Fuzzy Systems*, vol. 11, no. 3, pp. 354–360, 2003.

[23] M. S. Park and D. Chwa, "Swing-up and stabilization control of inverted-pendulum systems via coupled sliding-mode control method," *IEEE Transactions on Industrial Electronics*, vol. 56, no. 9, pp. 3541–3555, 2009.

[24] H. K. Khalil, *Nonlinear System*, Prentice Hall, Upper Saddle River, NJ, USA, 1996.